

Link Budget and Enhanced Communication Distance for Ambient Internet of Things



YANG Yibing¹, LIU Ming¹, XU Rongtao²,

WANG Gongpu¹, GONG Wei³

(1. School of Computer and Information Technology, Beijing Jiaotong University, Beijing 100044, China;

2. School of Electronic and Information Engineering, Beijing Jiaotong University, Beijing 100044, China;

3. School of Computer Science and Technology, University of Science and Technology of China, Hefei 230026, China)

DOI: 10.12142/ZTECOM.202401003

<https://kns.cnki.net/kcms/detail/34.1294.TN.20240223.1839.002.html>,
published online February 26, 2024

Manuscript received: 2023-12-02

Abstract: Backscatter communications will play an important role in connecting everything for beyond 5G (B5G) and 6G systems. One open challenge for backscatter communications is that the signals suffer a round-trip path loss so that the communication distance is short. In this paper, we first calculate the communication distance upper bounds for both uplink and downlink by measuring the tag sensitivity and reflection coefficient. It is found that the activation voltage of the envelope detection diode of the downlink tag is the main factor limiting the backscatter communication distance. Based on this analysis, we then propose to implement a low-noise amplifier (LNA) module before the envelope detection at the tag to enhance the incident signal strength. Our experimental results on the hardware platform show that our method can increase the downlink communication range by nearly 20 m.

Keywords: ambient IoT (AIoT); B5G; backscatter communication; link budget; low-noise amplifier (LNA); Release 19; tag chip sensitivity; upper bounds

Citation (Format 1): YANG Y B, LIU M, XU R T, et al. Link budget and enhanced communication distance for ambient Internet of Things [J]. *ZTE Communications*, 2024, 22(1): 16 - 23. DOI: 10.12142/ZTECOM.202401003

Citation (Format 2): Y. B. Yang, M. Liu, R. T. Xu, et al., "Link budget and enhanced communication distance for ambient Internet of Things," *ZTE Communications*, vol. 22, no. 1, pp. 16 - 23, Mar. 2024. doi: 10.12142/ZTECOM.202401003.

1 Introduction

Backscatter communications (BackCom), a key technology for ambient Internet of Things (AIoT), have the advantages of low hardware cost, low maintenance, easy deployment and flexible extension, and will play an important role in connecting everything for B5G and 6G systems. It was first introduced in the late 1940s by STOCKMAN^[1]. Afterward, the radio frequency identification (RFID)^[2] system enabled by BackCom has been widely used for commodity identification, item tracking, logistic management, etc. Recently, the third-generation partnership project (3GPP) started investigating the scenarios, use cases, services and targets of the potential use of BackCom in future wireless networks, and the corresponding network is referred to as ambient IoT^[3] in Release 19.

Different from traditional wireless communications, the

backscatter transmitters (e.g., tags, devices, and sensors) do not need to generate the carrier signal by itself. BackCom transmits information by reflecting the received RF signal in a modulated way. So, it leaves out the RF units of traditional communication equipment such as a local oscillator, a mixer, and a duplexer, which greatly simplifies the RF frontend and reduces the power consumption dedicated to RF signal transmission. As a consequence, backscatter devices do not need batteries but can accomplish wireless signal reception and transmission by wireless energy harvesting (EH) and BackCom, which significantly improves its sustainability^[4-6]. Therefore, BackCom has been regarded as a promising solution to passive and green IoT.

One open challenge for BackCom is that the signals suffer a round-trip path loss so that the communication distance is short, which is largely different from traditional point-to-point communications. Specifically, the signals in traditional point-to-point communication systems experience a one-way path loss, and both the transmitter and receiver are equipped with power amplifiers to enhance signal quality. As a result, it is relatively easier to achieve long-range communication. In con-

This work was supported in part by National Natural Science Foundation of China under Grant Nos. 61971029 and U22B2004, and in part by Beijing Municipal Natural Science Foundation under Grant No. L222002.

trast, in BackCom systems, the information is delivered through RF signal reflection. Therefore, the backscatter signals undergo a round-trip path loss, which requires a larger link budget. For example, the signal coverage of the ultra-high frequency (UHF) radio frequency identification (RFID) system, namely Electronic Product Code Global Class1 Generation 2 (EPC C1G2)^[7], is at the level of roughly 10 m in practical deployment, in comparison with coverage up to several hundred meters for typical cellular communication systems at the same frequency band with similar radiation power level. The communication range of BackCom could be further reduced if higher communication rates are required.

The short coverage inevitably limits the application of BackCom. Therefore, it is necessary to identify the major factors that restrict the communication range of BackCom systems and find corresponding effective solutions to boost its transmission capability. The major factors that constrain the communication distance may come from uplink or downlink. Accordingly, it is necessary to perform the link budget to calculate and compare the upper bound downlink and uplink communication distance.

Existing works have studied the link budget of BackCom mostly through theoretical analysis. Friis free-space formula was used to determine the theoretical upper bound communication distance in Refs. [8 – 9]. The authors in Ref. [10] incorporated more practical factors such as multipath propagation to derive more practical path losses of passive UHF tags. Four types of propagation models of BackCom were discussed in Ref. [11] and some insights into the link quality of BackCom transmission were provided.

Using the link budget, we can determine the power received at the tag and the reader. When the received power decreases to the sensitivity of the tag and the reader, we can calculate the upper bounds for the downlink and uplink communication distance. Next, comparing the two bounds, we can find the bottleneck of the BackCom, uplink or downlink. And the result is that BackCom is mainly limited by the downlink. Therefore, we need to improve the downlink sensitivity. That is, enhancing the tag sensitivity can increase the communication range of BackCom systems.

Generally speaking, the overall sensitivity of the tag is determined by the envelope detection circuit and the comparator. The sensitivity of the envelope detection circuit is related to the forward voltage drop of the diode. In order to improve the sensitivity, the authors in Ref. [12] suggested that the envelope detection circuit used diode-connected low positive channel Metal Oxide Semiconductor (PMOS) transistors for low-voltage operation and less energy loss. Ref. [13] introduced a detector-first wake-up receiver (WuRx) that used boundary condition-based envelope detector optimization, improving sensitivity and performance while conserving power. The envelope detector described in Ref. [14] employed the threshold compensation technology to effectively mitigate the

impact of the transistor's threshold voltage on demodulation sensitivity. A voltage doubler rectifier was proposed to improve the passive envelope detection of the tag, thereby enhancing the tag sensitivity^[15–16]. Unfortunately, when a multiple-stage voltage doubler rectifier is used, it is a challenge to design and implement the RF circuit. Besides, using a multiple-stage voltage doubler rectifier will cause annoying parasitic parameters that may lead to a relatively slower rectification rate.

Actually, the factors that can affect the tag sensitivity may be the forward voltage drop of the diode, the sensitivity of the comparator, and the algorithm limit imposed by the adopted decoding scheme. In summary, the bottleneck that restricts the communication range remains unclear and the results have not been validated over practical hardware implementations, which motivates our present work.

In this paper, we first derive the link budget of the BackCom transmission by taking into account practical factors including the impedance modulation mode, impedance matching, and polarization mismatch. Using the more comprehensive and accurate link budget model, the uplink and downlink communication ranges can be calculated with the nominal value of reader sensitivity and the measured tag sensitivity. It is found through the analysis that the key factor that sets the upper bound of our practical BackCom system is the capability of the envelope detection circuit of the downlink tags. To address this issue, we propose to incorporate a low-noise amplifier (LNA) module to enhance the signal strength before envelope detection, which consequently improves tag sensitivity and increases the communication distance of the downlink.

The remainder of this paper is organized as follows. Section 2 introduces two communication systems based on backscatter, then describes the downlink signal receiving and the uplink reflection signal process of the tag, and derives the reflection coefficient and radar cross section. In Section 3, firstly, the tag reflection coefficient and other parameters are measured to calculate the sensitivity. Secondly, through the received power and sensitivity, the upper bound distance between the upper and lower lines of the system is analyzed, and the upper bound of the system is obtained as the starting voltage of the diode of the label envelope detection module. Finally, a low-noise power amplifier module is implemented in the receiving circuit of the tag. In Section 4, the performance improvement of the communication system is verified through theoretical and practical measurements. Section 5 concludes the paper.

2 Backscatter Communication Model

Backscatter communication systems can be classified into two categories: monostatic backscatter communication systems (MBCS) and bistatic backscatter communication systems (BBCS)^[17], as shown in Figs. 1(a) and 1(b), respectively.

The MBCS in Fig. 1(a) illustrates that the RF carrier signal

transmitter and the backscatter signal receiver are collocated in one device commonly referred to as a reader. A typical reader may communicate with multiple backscatter tags in the surrounding area. The popular EPC C1G2 RFID system adopts this MBCS configuration.

In the downlink of MBCS, the reader broadcasts the RF carrier signal and signaling information simultaneously. The RF carrier signal can be leveraged by the tag to transmit its information back to the reader. The signaling information is used to activate specific tags and deliver associated commands. More specifically, the tag will be awakened and decode the signaling. Depending on signaling from the reader, the tag transmits its own information by reflecting and modulating the RF carrier signals^[18]. Consequently, the reader performs signal processing to the received backscatter signal to retrieve the tag information. It is worth noting that the backscattered signals that carry the tag information suffer from the power attenuation of both downlink and uplink.

As shown in Fig 1(b), the BBCS consists of three components: a backscatter reader, a tag, and an RF carrier source. In comparison with MBCS, BBCS separates the RF carrier source functionality from the backscatter signaling and information transceiver. This can not only offer flexibility to the practical deployment but improve the signal strength at the reader. The backscatter signal received by the reader also undergoes the path loss of both uplink and downlink. Whereas, since the RF carrier source and the reader are not necessarily collocated and the former can be close to the tag, the incident signal power at the tag antenna in BBCS can be higher than that in MBCS.

Instead of generating an active RF signal in traditional wireless communication systems, the tag in MBCS and BBCS controls and changes the load impedance of the antenna to modulate the incident carrier signals. This yields the RF carrier reflected from the tag antenna in an alternating manner. The tag can encode its information by properly controlling the changing pattern of the reflected signal. The reader, on the other hand, can retrieve the information from the tag by observing the variation of the backscatter signal.

Let Z_a denote the complex tag antenna impedance of the tag

antenna. The reflection coefficient of the tag antenna can be expressed as:

$$\Gamma = \frac{Z_c - Z_a^*}{Z_c + Z_a^*}, \quad (1)$$

where Z_c is the complex load impedance. When $\Gamma = 0$ ($Z_c = Z_a^*$), it is called the impedance matching state or the impedance absorption state, and the tag does not generate any reflected signals. When $\Gamma \neq 0$, the tag modulates the impedance of load to alter the reflection coefficient, thereby causing changes in the amplitude and phase of the reflected signals. This process is known as the impedance modulation, and the alteration of the reflected signal is detectable and decodable into data by the reader.

The process of impedance modulation is analogous to target identification in radar systems, where the radar cross section (RCS) serves as a metric to quantify the target's ability to reflect radar waves. By considering the tag as the target for assessing its reflective capability, we can express the tag antenna RCS^[19] as follows:

$$\sigma_i = \frac{\lambda^2 G_{\text{tag}}^2}{4\pi} |\Gamma_i - A_s|^2, \quad (2)$$

where λ is the wavelength and G_{tag} is the tag antenna gain. Tag RCS affects the field backscattered from a loaded antenna RCS. It can be divided into load-dependent and load-independent components. The subscript i indicates that the load Z_{ci} is connected to the tag antenna, corresponding to the reflection coefficient Γ_i . For example, when there are only two load states, $i = 1$ is for the tag information bit "0" and $i = 2$ is for the tag information bit "1". A_s corresponds to the structural mode of the tag antenna, which is a load-independent antenna characteristic. Its value is complex, in general, and depends on the geometry and materials used for the antenna construction.

The tag modulates its information by changing the RCS, and the modulated backscatter signal is proportional to the difference of tag RCS ($\Delta\sigma$). Furthermore, the magnitude of $\Delta\sigma$ is shown as below.

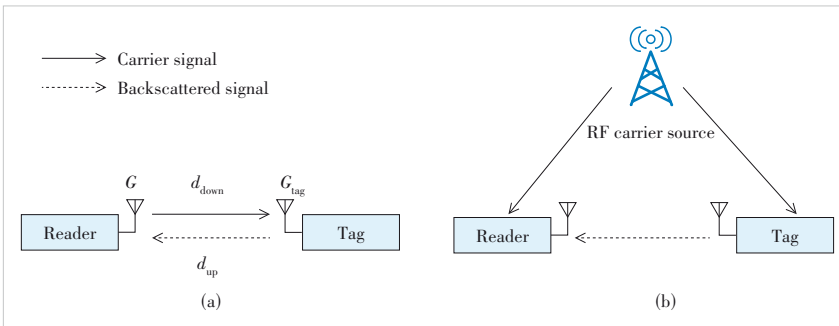
$$\Delta\sigma = \frac{\lambda^2 G_{\text{tag}}^2}{4\pi} \alpha |\Gamma_1 - \Gamma_2|^2, \quad (3)$$

where the coefficient α depends on the tag's modulation system. When the duty cycle of the tag's square-wave modulated signal is 50%, we can have $\alpha=1/4$ ^[20].

3 Link Budget

3.1 Downlink Budget

In the downlink communication, the reader



▲ Figure 1. Two backscatter communication systems: (a) monostatic backscatter communication system and (b) bistatic backscatter communication system

generates and broadcasts signaling that includes reflection indication information to activate the tag. Note that the signal strength is a critical parameter to evaluate the reliability of data transmission. Therefore we use effective isotropic radiated power (EIRP), a value that measures the coverage range and communication capability of a wireless system. The transmitted EIRP of the reader can be expressed as:

$$\text{EIRP}_t = P_t G, \quad (4)$$

where P_t represents the transmission power used by the reader, which indicates the actual power output from the transmitter to the antenna, and G is the gain of the reader antenna, which is the efficiency of the antenna relative to an ideal isotropic antenna. The higher the EIRP, the stronger the transmission capability of the system, allowing it to propagate over longer distances.

In a multipath environment, the path loss between the reader and the tag antennas can be written as^[10]

$$L_p(d) = \left(\frac{\lambda}{4\pi d} \right)^2 \left| 1 + \sum_{n=1}^N \Gamma_n \frac{d}{d_n} e^{-jk(d_n - d)} \right|^2, \quad (5)$$

where d is the length of the direct path, and d_n is the length of the n -th path with a reflection coefficient of Γ_n . N is the total number of reflections.

The signal strength at the tag antenna location can be obtained from the transmitted EIRP and path loss as follows:

$$P_{\text{tag}} = \text{EIRP}_t G_{\text{tag}} \beta L_p(d_{\text{down}}) = P_t G G_{\text{tag}} \beta L_p(d_{\text{down}}), \quad (6)$$

where β is the polarization mismatch, also known as polarization isolation, which measures the degree of signal loss caused by polarization mismatch in signal transmission from the reader antenna to the tag antenna. G_{tag} is the gain of the tag antenna, and d_{down} is the downlink communication distance.

As shown in Fig. 2, the signal received from the tag antenna will go through the impedance matching circuit. Since the reflection coefficient is usually not equal to 0, a small part of the signal will be reflected by the tag antenna. The signal that is

eventually captured and processed by the signal reception circuit of the tag is:

$$P_{\text{tag, chip}} = P_{\text{tag}} (1 - |\Gamma|^2), \quad (7)$$

where Γ is the reflection coefficient of impedance matching. The power reflection coefficient $|\Gamma|^2$ shows the fraction of the maximum power available from the generator that is not delivered to the load^[8]. A well-designed impedance matching is of vital importance to the system performance. The impedance matching circuit is normally designed to achieve $\Gamma = 0$ to maximize the signal reception.

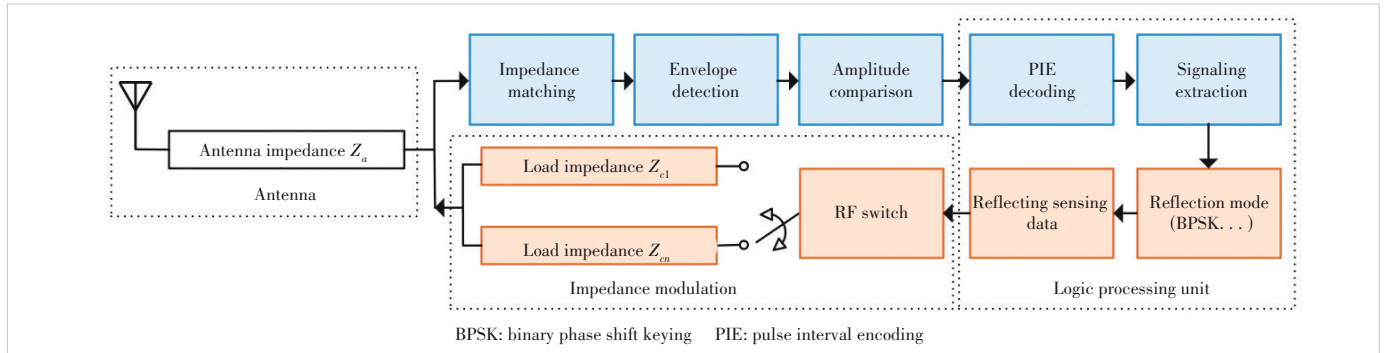
After that, the received signal is processed by the envelope detection module for demodulation. It converts the received RF signal into a low-frequency envelope signal with varying amplitudes. The following comparison module calculates a threshold based on the long-term average value of the varying envelope, and determines the information carried on the envelope by comparing the instantaneous envelope with the threshold. Subsequently, the bi-level output is processed by the logic processing unit. Consequently, the tag extracts control information such as the reflection rate and the modulation scheme from the decoded sequence. With this information, the tag specifies its working mode and prepares the signal transmission that will be carried out later.

3.2 Uplink Budget

In uplink communications, the tag modulates and reflects its information through impedance modulation. The reader processes the received reflected signal. The tag modulates and reflects a modulated backscatter signal with differential EIRP (ΔEIRP). The backscattered power of the tag can be calculated as $\Delta\text{EIRP} = S\Delta\sigma$. The following equation exhibits a proportional relationship with the received power P_{tag} ^[21]:

$$\frac{\Delta\text{EIRP}}{P_{\text{tag}}} = \frac{S\Delta\sigma}{SA} = G_{\text{tag}} K, \quad (8)$$

where $K = \alpha |\Gamma_1 - \Gamma_2|^2$ represents the tag modulation loss factor. S is the power density of an electromagnetic (EM) wave



▲ Figure 2. Typical functional diagram inside a tag

incident on the tag. $A = \frac{\lambda^2 G_{\text{tag}}}{4\pi}$ is the effective area of the tag antenna.

The power of the modulated tag signal received by reader antennas can be written in terms of differential EIRP as

$$P_r = \Delta \text{EIRP} G \beta L_p(d_{\text{up}}) = P_{\text{tag}} G_{\text{tag}} K G \beta L_p(d_{\text{up}}) = P_t G^2 G_{\text{tag}}^2 \beta^2 L_p(d_{\text{down}}) L_p(d_{\text{up}}) \alpha |\Gamma_1 - \Gamma_2|^2, \quad (9)$$

where d_{down} is the downlink communication distance. It can be observed that the signal received by the reader undergoes path loss in both the uplink and downlink. Based on the analysis of the sensitivity and received power at readers and tags, respectively, which is conducted in the next section, it can be seen that the limiting bottleneck for the communication distance of MBCS is the downlink communication distance.

4 Downlink Improvement of Tag

4.1 Tag Chip Sensitivity

In downlink communications, the tag receives and extracts the signaling indication information of RF signals sent from the reader, and sets the corresponding reflection mode. However, signal decoding and information extraction from RF signals can be implemented by an analog-to-digital converter (ADC), as in traditional wireless systems. However, it consumes a significant amount of power and therefore is not suitable for ultra-low power systems. In a signal reception module of the tag, a threshold comparison circuit with lower power consumption is used to achieve frequency down-conversion.

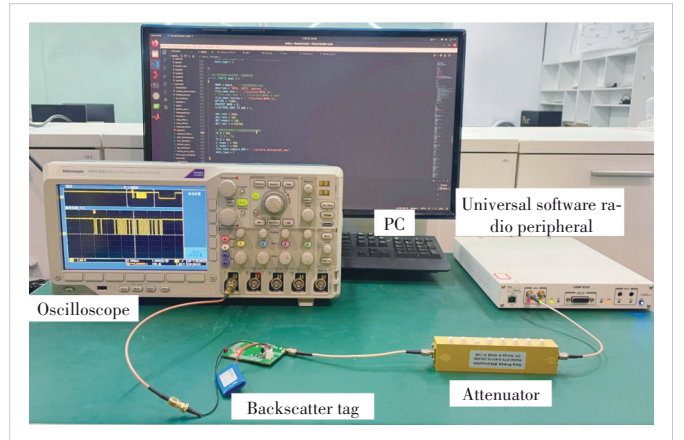
The tag chip sensitivity is also known as the activation threshold, indicating the minimum power of signaling that can be recognized by the tag's logic processing unit and used to perform impedance modulation. Depending on the tag's reception processing, factors affecting sensitivity may be the forward voltage drop of the diode, the sensitivity of the comparator, and the algorithm limit imposed by the adopted decoding scheme.

More specifically, if the input signal is lower than the level of forward voltage drop, the received signal cannot be demodulated and no output will be generated. Similarly, when the input signal is too weak, the signal amplitudes that represent different information states are very close to each other. Especially, when the difference is lower than the minimum difference that can be detected by the comparator (i.e. the sensitivity of the comparator), the comparator cannot output reliable results for the following processing. In addition, the decoding algorithm employed by the tag may also have certain performance upper bound, beyond which the decoding algorithm cannot constantly provide correct output information. This performance upper bound is usually associated with the signal quality.

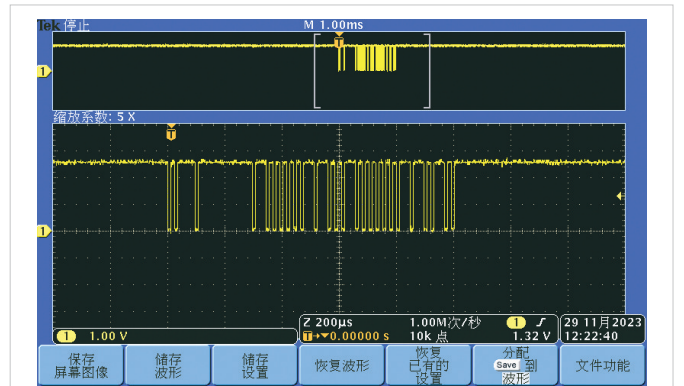
We measure the chip sensitivity of the tag with the following experiments. As shown in Fig. 3, we use universal software radio peripheral (USRP) to transmit a carrier signal and signaling with certain power, through an attenuator connected to the tag, and connect the comparator output of the tag to an oscilloscope. The operating frequency is 925 MHz, and the measurement steps are as follows. Firstly, we measure the threshold power P_{th} at the tag antenna when the comparator has a stable waveform output corresponding to the signaling. That is, the tag correctly decodes the signaling and initiates reflection. Fig. 4 shows the comparator's output waveform measured by the oscilloscope at $P_{\text{th}} = -19.90$ dBm, matching the signaling from the reader. Due to an increase in the attenuation value of the attenuator, the comparator waveforms no longer match. The threshold power P_{th} is called the tag sensitivity. Secondly, the reflection coefficient $|\Gamma| = 0.1384$ of impedance matching is measured by using a vector network analyzer (VNA) at the P_{th} power level. The tag chip sensitivity $P_{\text{chip, sen}} = -19.98$ dBm.

4.2 Communication Distance Upper Bound

In MBCS, when $L_p(d_M) = \left(\frac{\lambda}{4\pi d_M}\right)^2$, the upper bound of the downlink distance can be determined by:



▲ Figure 3. Sensitivity measurement experiment



▲ Figure 4. Output waveform of the comparator

$$d_{\text{down}} = \frac{\lambda}{4\pi} \sqrt{\frac{P_t G G_{\text{tag}} \beta (1 - |\Gamma|^2)}{P_{\text{tag,chip}}}} \quad (10)$$

Similarly, the upper bound of the uplink distance is

$$d_{\text{up}} = \frac{\lambda}{4\pi} \sqrt[4]{\frac{P_t G^2 G_{\text{tag}}^2 \beta^2 \alpha |\Gamma_1 - \Gamma_2|^2}{P_r}} \quad (11)$$

We set the reader sensitivity $P_{\text{reader, sen}} \approx -86$ dBm, the reader antenna gain $G = 5$ dBi, the tag antenna gain $G_{\text{tag}} = 2$ dBi, polarization mismatch $\beta = 0.5$, and coefficient $\alpha = 1$ ^[22].

Suppose that the tag adopts the binary phase shift keying (BPSK) modulation mode. Due to the influence of factors such as RF switch and transmission line impedance, the actual reflection coefficient is often less than 1. When the tag adopts the BPSK modulation, the values of the measured reflection coefficients are $\Gamma_1 = -0.69 + 0.32j$ and $\Gamma_2 = 0.67 - 0.23j$, respectively. Figs. 5 and 6 are respectively signal power received by the tag chip and the reader when transmission power of the reader $P_t = 10, 15$ and 20 dBm, respectively.

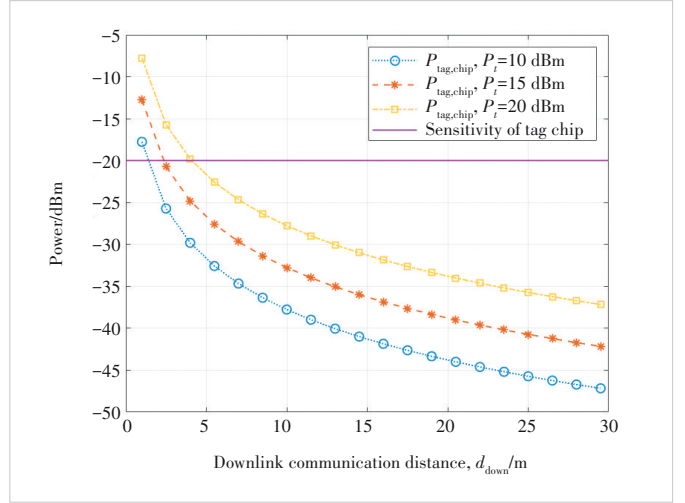
When the tag chip received power equals to the envelope detection threshold power ($P_{\text{tag,chip}} = P_{\text{chip, sen}}$), the downlink upper bound communication distance $d_{\text{down}} \approx 2.30$ m. Similarly, when $P_r = P_{\text{reader, sen}}$, the uplink upper bound communication distance $d_{\text{up}} \approx 16.76$ m. Final upper bound communication distance $d_M = \min\{d_{\text{down}}, d_{\text{up}}\} = 2.30$ m. In the real-world test, the restriction of the software program on the signaling preamble is reduced, and the tag cannot receive signaling information when approaching the upper bound distance. At this time there is no comparison voltage output from the viewing comparator and envelope signal output from the envelope detection. Accordingly, we conclude that the downlink distance is mainly limited by the envelope detection threshold.

Based on the previous measurements and analysis, we propose to implement an LNA module after the tag antenna reception. As shown in Fig. 7, the added LNA amplifies the strength of the signal received by the tag while minimizing the noise in the signal to ensure that the signal-to-noise ratio (SNR) can be maintained at a high level when the signal is transmitted and processed in the system. Since the LNA amplifies the voltage input to the envelope detection, the tag is easier to detect the downlink signaling. The gain of LNA

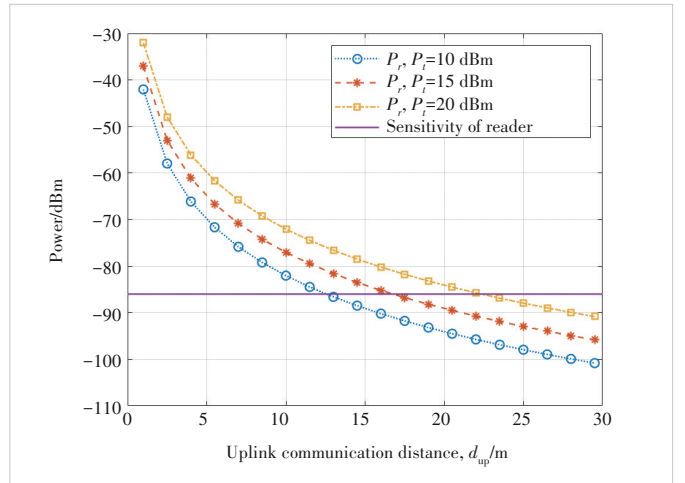
$G_{\text{LNA}} = 21$ dB. The tag chip sensitivity remains unchanged, but the threshold power $P_{\text{th, LNA}}$ at the arrival of the tag antenna decreases to $P_{\text{th}} - G_{\text{LNA}}$. Eventually, the sensitivity of the labels is roughly improved by G_{LNA} .

5 Performance Analysis

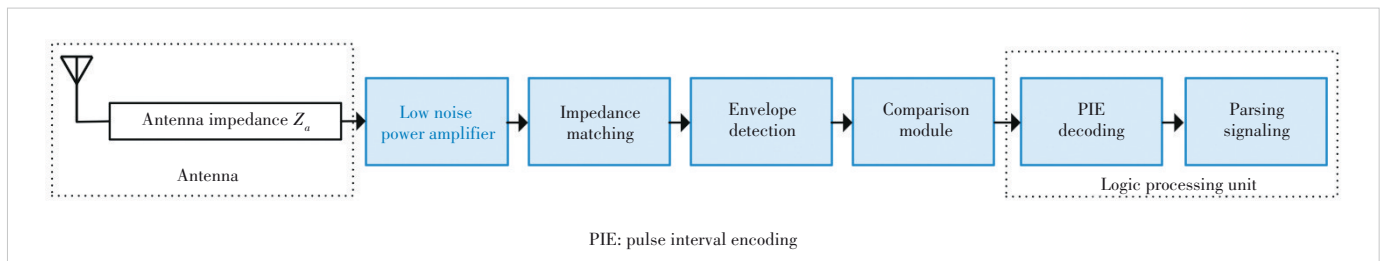
The signal power $P_{\text{tag,chip}}$ and $P_{\text{tag,chip, LNA}}$ received by tag chips versus the distance are plotted in Fig. 8, where the transmission power of the reader is set as $P_t = 15$ dBm. We use the



▲ Figure 5. Signal power received at the tag



▲ Figure 6. Signal power received by the reader

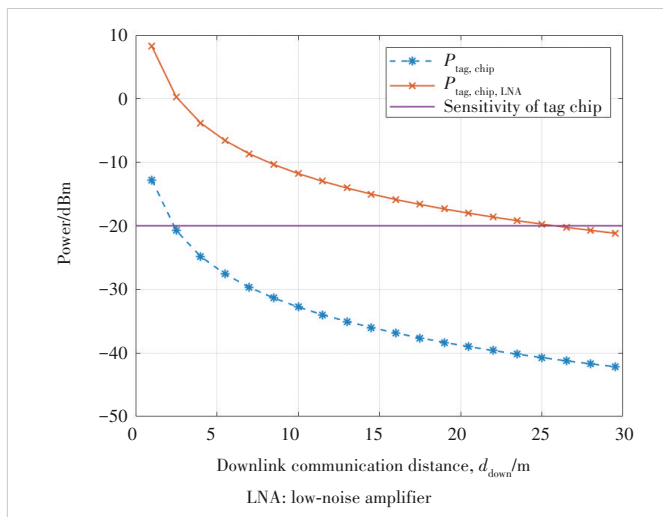


▲ Figure 7. Functional diagram of the backscatter tag with enhanced downlink

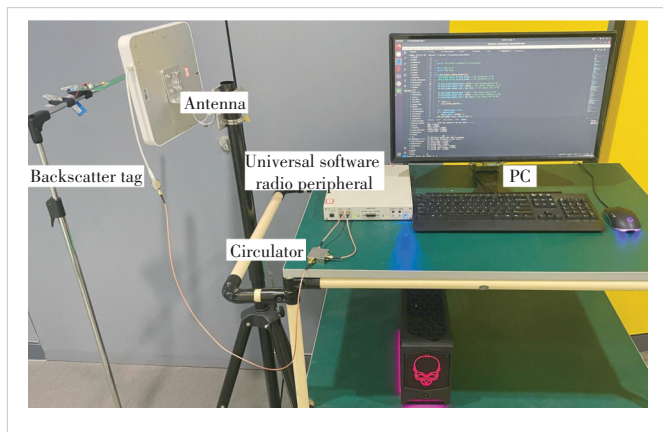
same configuration as those in Fig. 5.

When $P_{\text{tag,chip,LNA}} = P_{\text{chip,sen}}$, we can obtain that the upper bound of downlink communication distance can be 25.75 m, i. e., $d_{\text{down,LNA}} \approx 25.75$ m. After implementing the LNA, the downlink upper bound communication range is improved by 23.45 m.

The test environment is depicted in Fig. 9, where a USRP is in conjunction with a PC as an integrated system. The USRP is typically used as the radio front-end hardware, responsible for receiving and transmitting radio signals. The PC is used for processing and analyzing these received signals. The transmission and reception of radio frequency signals are realized by connecting the antenna with a circulator. The operating frequency is 925 MHz, and the transmission power $P_t = 15$ dBm. We measure the upper bound distance as the maximum distance at which the tag can correctly recognize the signaling. Our final measurement results indicate that, after implementing the LNA module, the communication range is increased by approximately 20 m.



▲ Figure 8. Signal power received at the tag



▲ Figure 9. Downlink upper bound communication distance measurement experiment

In MBCS, the tag can identify smaller signals after implementing the LNA module. According to our analysis, the downlink sensitivity is the bottleneck that sets the upper bounds of the overall communication range. The improvement in the downlink communication distance consequently leads to an improved uplink distance, lower reader power consumption and enhanced communication performance. It is worth noting that these benefits can also be achieved in some BBCS configurations. Improving tag sensitivity will result in an extended maximum effective communication distance between the RF carrier source and the tag.

6 Conclusions

In this paper, we analyze the uplink and downlink budgets and measure the chip sensitivity of the tag for ambient IoT. According to the relationship between sensitivity and the received power, we derive the upper bounds of both uplink and downlink distances. It is found that the backscatter communications are mainly limited by the downlink distance, instead of the uplink distance. It is also found that the tag sensitivity results from its hardware constraints, especially the activation voltage of the envelope detection diode. Accordingly, we propose to incorporate an LNA in the tag to amplify the incident signals before the envelope detection, and the corresponding experimental results show that the downlink communication range could be extended over 20 m.

References

- [1] STOCKMAN H. Communication by means of reflected power [J]. Proceedings of the IRE, 1948, 36(10): 1196 - 1204. DOI: 10.1109/JRPROC.1948.226245
- [2] ROY S, JANDHYALA V, SMITH J R, et al. RFID: from supply chains to sensor nets [J]. Proceedings of the IEEE, 2010, 98(9): 1583 - 1592. DOI: 10.1109/jproc.2010.2053690
- [3] 3GPP. Study on Ambient IoT (Internet of Things) in RAN: TR 38.848 [S]. 2023
- [4] LIU X L, ANSARI N. Toward green IoT: energy solutions and key challenges [J]. IEEE communications magazine, 2019, 57(3): 104 - 110. DOI: 10.1109/MCOM.2019.1800175
- [5] TORO U S, WU K S, LEUNG V C M. Backscatter wireless communications and sensing in green Internet of Things [J]. IEEE transactions on green communications and networking, 2022, 6(1): 37 - 55. DOI: 10.1109/TGCN.2021.3095792
- [6] SONG C Y, DING Y, EID A, et al. Advances in wirelessly powered backscatter communications: from antenna/RF circuitry design to printed flexible electronics [J]. Proceedings of the IEEE, 2022, 110(1): 171 - 192. DOI: 10.1109/JPROC.2021.3125285
- [7] EPCglobal. EPC radio-frequency identity protocols Class-1 Generation-2 UHF RFID protocol for communications at 860 MHz-960 MHz: GB3100-3102 [S]. 2015
- [8] NIKITIN P V, RAO K V S, LAM S F, et al. Power reflection coefficient analysis for complex impedances in RFID tag design [J]. IEEE transactions on microwave theory and techniques, 2005, 53(9): 2721 - 2725. DOI: 10.1109/TMTT.2005.854191
- [9] DE VITA G, IANNACONE G. Design criteria for the RF section of UHF

- and microwave passive RFID transponders [J]. *IEEE transactions on microwave theory and techniques*, 2005, 53(9): 2978 - 2990. DOI: 10.1109/TMTT.2005.854229
- [10] LAZARO A, GIRBAU D, SALINAS D. Radio link budgets for UHF RFID on multipath environments [J]. *IEEE transactions on antennas and propagation*, 2009, 57(4): 1241 - 1251. DOI: 10.1109/TAP.2009.2015818
- [11] GRIFFIN J D, DURGIN G D. Complete link budgets for backscatter-radio and RFID systems [J]. *IEEE antennas and propagation magazine*, 2009, 51(2): 11 - 25. DOI: 10.1109/MAP.2009.5162013
- [12] WEI P, CHE W Y, BI Z Y, et al. High-efficiency differential RF front-end for a Gen2 RFID tag [J]. *IEEE transactions on circuits and systems II: Express briefs*, 2011, 58(4): 189 - 194. DOI: 10.1109/TCSII.2011.2124530
- [13] MOODY J, BASSIRIAN P, ROY A, et al. Interference robust detector-first near-zero power wake-up receiver [J]. *IEEE journal of solid-state circuits*, 2019, 54(8): 2149 - 2162. DOI: 10.1109/JSSC.2019.2912710
- [14] TIAN Y, YU N, LI J, et al. A high sensitivity and high dynamic range ASK demodulator for passive UHF RFID with over-voltage protection [C]//International conference on electronics technology. IEEE, 2023: 1012 - 1016. DOI: 10.1109/ICET58434.2023.10211808
- [15] MOODY J, BASSIRIAN P, ROY A, et al. A -76 dBm 7.4 nW wakeup radio with automatic offset compensation [C]//IEEE International Solid-State Circuits Conference. IEEE, 2018: 452 - 454. DOI: 10.1109/ISSCC.2018.8310379
- [16] ALAJI I, AOUIMEUR W, GHANEM H, et al. Design of zero bias power detectors towards power consumption optimization in 5G devices [J]. *Microelectronics journal*, 2021, 111: 105035. DOI: 10.1016/j.mejo.2021.105035
- [17] KIMIONIS J, BLETSAS A, SAHALOS J N. Increased range bistatic scatter radio [J]. *IEEE transactions on communications*, 2014, 62(3): 1091 - 1104. DOI: 10.1109/TCOMM.2014.020314.130559
- [18] DOBKIN D M. *The RF in RFID* [M]. Amsterdam, Netherlands: Elsevier, 2008. DOI: 10.1016/B978-0-7506-8209-1.X5001-3
- [19] GREEN R B. *The general theory of antenna scattering* [D]. Columbus, USA: The Ohio State University, 1963
- [20] NIKITIN P V, RAO K V S. Antennas and propagation in UHF RFID systems [C]//IEEE International Conference on RFID. IEEE, 2008: 277 - 288. DOI: 10.1109/RFID.2008.4519368
- [21] NIKITIN P V, RAO K V S. Theory and measurement of backscattering from RFID tags [J]. *IEEE antennas and propagation magazine*, 2006, 48(6): 212 - 218. DOI: 10.1109/MAP.2006.323323
- [22] NIKITIN P V, RAO K V S, MARTINEZ R D. Differential RCS of RFID tag [J]. *Electronics letters*, 2007, 43(8): 431. DOI: 10.1049/el: 20070253

Biographies

YANG Yibing received her BS degree from Anhui University, China in 2022. She is currently working toward her PhD degree with the School of Computer Science and Technology, Beijing Jiaotong University, China. Her research interests include mobile and Internet networks

LIU Ming (mingliu@bjtu.edu.cn) received his BE and ME degrees in electrical engineering from Xi'an Jiaotong University, China in 2004 and 2007, respectively, and PhD degree in electrical engineering from the National Institute of Applied Sciences, France in 2011. He was with the Institute of Electronics and Telecommunications of Rennes, France, as a postdoctoral researcher from 2011 to 2015. He is currently with Beijing Jiaotong University, China, as an associate professor. His main research interests include beyond 5G/6G, PHY security, and AI for wireless communications.

XU Rongtao received his BS degree in radio technology from Xi'an Jiaotong University, China in 1997, MS degree in communication and information system from the Beijing University of Posts and Telecommunications, China in 2000, and PhD degree in electronic and information engineering from The Hong Kong Polytechnic University, China in 2007. From 2000 to 2003, he was a system engineer at Siemens Ltd., China. In 2007, he joined Beijing Jiaotong University, China, where he is currently an associate professor with the State Key Laboratory of Rail Traffic Control and Safety. His research interests include wideband mobile communications, railway communications, and wireless sensor networks.

WANG Gongpu received his BE degree in communication engineering from Anhui University, China in 2001, MS degree from the Beijing University of Posts and Telecommunications, China in 2004, and the PhD degree from University of Alberta, Canada in 2011. From 2004 to 2007, he was an assistant professor at the School of Network Education, Beijing University of Posts and Telecommunications. He is currently a full professor with the School of Computer and Information Technology, Beijing Jiaotong University, China. His research interests include wireless communication theory, signal processing technologies, and the Internet of Things.

GONG Wei received his BE degree in computer science from Huazhong University of Science and Technology, China, and ME degree in software engineering and PhD degree in computer science from Tsinghua University, China. He is a professor with the School of Computer Science and Technology, University of Science and Technology of China. He had also conducted research with Simon Fraser University, Canada, and the University of Ottawa, Canada. His current research interests include wireless networks, Internet of Things, and distributed computing.